

# Vehicle-to-Vehicle Visible Light Communication: How to select receiver locations for optimal performance?

Hossien B. Eldeeb and Murat Uysal

Department of Electrical and Electronics Engineering

Özyeğin University, Istanbul, Turkey, 34794

## Abstract

Visible light communication (VLC) utilizes vehicle headlights as wireless transmitters and has emerged as a strong candidate for vehicle-to-vehicle (V2V) communications. In majority of works on V2V VLC systems, a common underlying assumption is that two vehicles within the same lane follow each other in a perfect alignment. In practical scenarios, a precise alignment is not available between two vehicles even if they are in the same lane. In this paper, we consider a VLC-based V2V system where the destination vehicle is equipped with four photodetectors for an omni-directional coverage. We use ray tracing simulations for channel modelling and calculate the received power for practical cases with imperfect alignment between two vehicles. In addition, we investigate the performance for lane changes. Our simulation results provide insight into which photodetectors are essential for each scenario under consideration.

## 1. Introduction

Visible light communication utilizes light emitting diodes (LEDs) as wireless transmitters without any adverse effect on illumination levels [1]. VLC was originally proposed as an indoor wireless access technology to take advantage of the existing illumination infrastructure. The increasing adoption of LED-based headlamps and taillights as well as the availability of LED-based street and traffic lights makes VLC also a strong candidate for vehicle-to-vehicle (V2V) and vehicle-to-infrastructure (V2I) communications [2, 3].

As in any other communication system, channel modeling is critical for link budget calculations and optimized system design for vehicular VLC [4]. Initial works in the related literature have made some ideal, yet unrealistic assumptions. For example, a common assumption [5-7] is the Lambertian illumination pattern of light source. Such a pattern might be valid for indoor light sources but cannot be used to model the asymmetrical intensity distribution of vehicle headlights. Another overlooked issue is road reflectance and its effect has been studied only in some recent works [8, 9]. Since vehicular VLC systems operate in outdoor medium, their performance in adverse weather conditions such as rain and fog are also important. These have been further investigated in [10, 11].

In majority of works on V2V VLC systems, a common underlying assumption is that two vehicles within the same lane follow each other in a perfect alignment. It is also commonly assumed that there are one or two photodetectors placed at the

back of the preceding car. In practical scenarios, it is obvious that there will not be a precise alignment between two vehicles even if they are in the same lane. Similarly, it is important to maintain connectivity while changing a lane. In this context, a major design challenge is how to select a minimum number of photodetectors (receivers) with proper locations to achieve a reliable communication in such practical scenarios.

In this paper, we attempt to answer this fundamental question through realistic channel modeling of VLC-based V2V link. The source destination uses high-beam headlights as its transmitters. We assume that the destination vehicle is equipped with four PDs. The first two PDs are located at the back of the vehicle under taillights. The other two PDs are located at the vehicle-sides below the mirrors, one at the left side and the second at the right one. Specifically, we consider three scenarios: 1) As a benchmark, we consider the commonly assumed scenario where two vehicles within the same lane follow each other at a constant speed with perfect alignment. 2) In the second scenario, two vehicles move in the same lane, but are not strictly aligned. We assume a horizontal shift between two vehicles. 3) In the third scenario, the source vehicle changes its lane while communicating with the destination vehicle in the target lane. We run ray tracing simulations to obtain channel impulse response (CIR) for these scenarios. Based on these CIRs, the total received optical power and the power percentage of each PD are calculated. These provide insight into which PDs are essential for each scenario under consideration.

The rest of the paper is organized as follows. In Section II, we describe our channel modeling approach based on non-sequential ray tracing. In Section III, we present the simulations for V2V scenarios. First, we calculate the received power using each individual PD. Then, we present the total contribution of received optical power considering all PDs under consideration. In last part of this section, we introduce the power percentage of each PD along the whole inter-vehicle distance under consideration. Finally, we provide concluding remarks in Section VI.

## 2. Channel Modeling Approach and System Model

For channel modeling, we use built-in non-sequential ray tracing feature of the optic system design software Zemax®. This modeling approach was first used to model indoor VLC channels [12] and also applied to V2V channels in [9, 11]. As illustrated in Fig. 1, we consider three V2V scenarios in a two-lane highway road, each has a lane width of 3.75 m [13, 14]. In Scenario I, we assume that two vehicles are located at the center

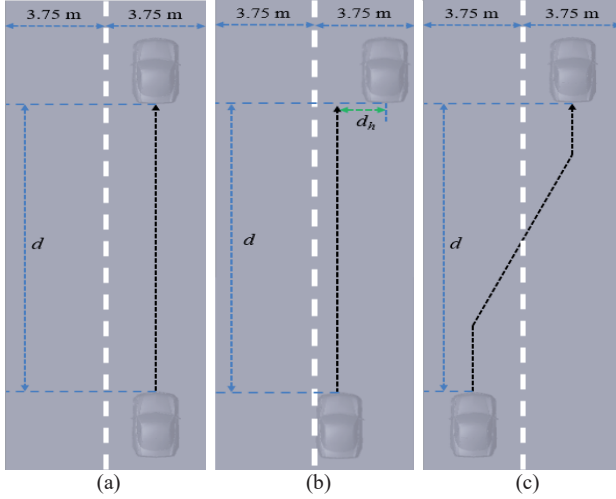


Fig. 1. V2V scenarios under consideration. (a) Scenario I (b) Scenario II (c) Scenario III.

of the same lane (perfectly aligned) and separated with an inter-vehicle distance of  $d$  as shown in Fig. 1(a). In scenario II, we assume that the two vehicles travel in the same lane however there is a misalignment (represented by  $d_h$ ) between the two vehicles, see Fig. 1(b). In Scenario III, the driver of the source vehicle starts to change his/her current lane and aims to maintain connectivity with the destination vehicle through this lane change as shown in Fig. 1(c).

First, we create the 3D simulation environment in Zemax. Following the specifications of [9], we assume “R2” type asphalt road which exhibits mixed diffuse and specular reflection. As illustrated in Fig. 2, we assume that vehicles have black color and are modeled as CAD objects with dimensions of  $4.67 \text{ m} \times 1.85 \text{ m} \times 1.37 \text{ m}$ . Headlamps of the source vehicle serve as wireless transmitters. The destination vehicle is equipped with four PDs. The first two PDs (denoted by PD 1 and PD 2) are located at the back of the vehicle under taillights. The other two PDs (denoted by PD 3 and PD 4) are located at the sides of vehicles below the mirrors at typical location of car crash sensor. A summary of simulation parameters is provided in Table I.

Using non-sequential ray tracing of Zemax®, the received optical power, the path length, and the propagation delay for each ray reaching to the PDs are computed. For a given distance, let  $P_{ij}$  and  $\tau_{ij}$  respectively denote the optical power and the propagation delay of the  $i^{\text{th}}$  ray received by the  $j^{\text{th}}$  PD,  $j = 1, \dots, 4$ . The CIR associated with the  $j^{\text{th}}$  PD can be therefore written as

$$h_j(t) = \sum_{i=1}^{N_j} P_{ij} \delta(t - \tau_{ij}). \quad (1)$$

where  $\delta$  is the Dirac delta function and  $N_j$  is the number of rays that reach the  $j^{\text{th}}$  PD. In simulations, we assume that the total optical power of two headlights (serving as transmitters) is unity. We can then scale the CIR for any given value of transmit power  $P_t$ . The received power can be therefore calculated as  $P_{r,j} = P_t H_j$  where  $H_j = \int_0^\infty h_j(t) dt$  is the channel DC gain associated with the  $j^{\text{th}}$  PD. The total power can be simply calculated as  $P_r = \sum_{j=1}^4 P_{r,j}$ .



Fig. 2. Locations of high-beam headlights (transmitters) and photodetectors (receivers) on the vehicles.

TABLE I. Simulation parameters

Transmitter specifications	Type: Brand: Power (Pt):	Philips Luxeon white light high-beam headlamp 1 W (normalized)
Receiver specifications	Area: FOV:	1 cm <sup>2</sup> 180°
Road specifications	Type: Material: Lane width:	R2 Asphalt 3.75 m
Car specifications	Length: Width: Height: Material:	4.67 m 1.85 m 1.37 m Black gloss paint

### 3. Simulation of V2V Scenarios

In this section, we first demonstrate the received optical power with respect to the inter-vehicle distance of  $d$  considering the total contribution of all PDs under consideration. Then, we present the power percentage of each PD along the whole inter-vehicle distance for all scenarios under consideration.

In Fig. 3, we consider scenario II and investigate the effect of misalignment between the vehicles. As a benchmark, perfect alignment scenario (Scenario I) is included. It is observed that the received power reduces when the horizontal displacement increases. For example, consider  $d = 10 \text{ m}$ . The received power when the two vehicles are perfectly aligned ( $d_h = 0 \text{ m}$ ) is  $-41.4 \text{ dB}$ . This reduces to  $-42.4 \text{ dB}$  and  $-43.6 \text{ dB}$  for  $d_h = 1 \text{ m}$  and  $d_h = 2 \text{ m}$ , respectively.

In order to identify which PDs contribute at what extent to total received power, we present pie charts in Fig. 4. It is observed that, in the perfect alignment case, PD1 and PD2 have almost identical shares. Only a very small received power is collected by PD3 and PD4 as a result of reflections. When there is some displacement (to the left-hand side) between two vehicles, it is observed that PD3 (located on left hand side of the destination vehicle) is now able to collect a significant amount of received power. On the other hand, the received power using PD 4 (located on right hand side of destination vehicle) is much reduced due to its location on the other side of displacement.

In Fig. 5, we consider lane changing scenario, i.e. Scenario III. In this scenario, we consider two cases: In the first case (Case A), the source vehicle is located at the center of the lane when it starts to change its lane. In the second case (Case B), the source vehicle is located at the edge of the lane at the start of the lane change process. We assume that the source vehicle starts to change its lane at  $d = 30 \text{ m}$  and ends this process at  $d = 15 \text{ m}$ . It

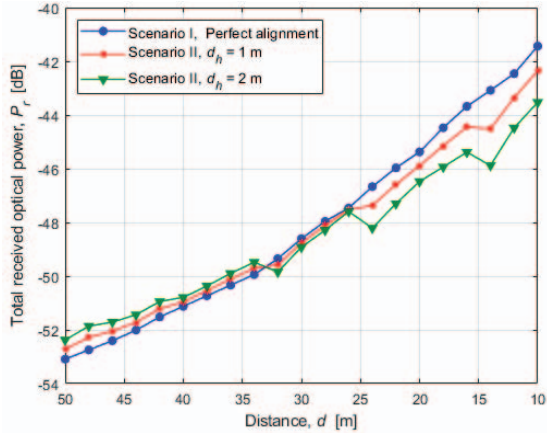


Fig. 3. Received optical power for scenario II (Effect of horizontal displacement).

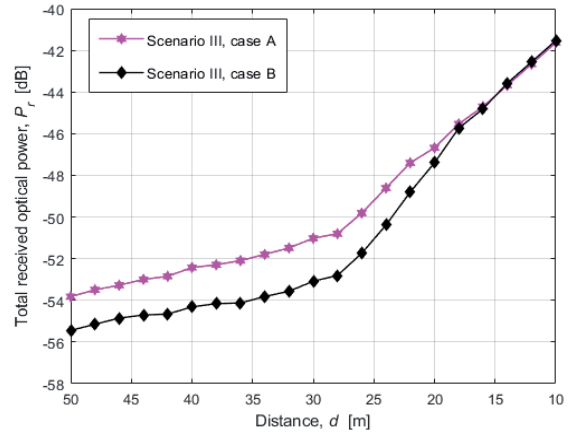
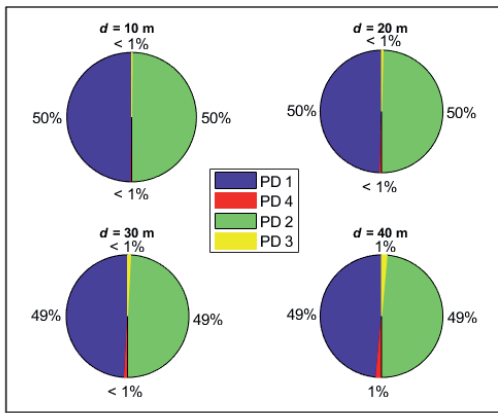
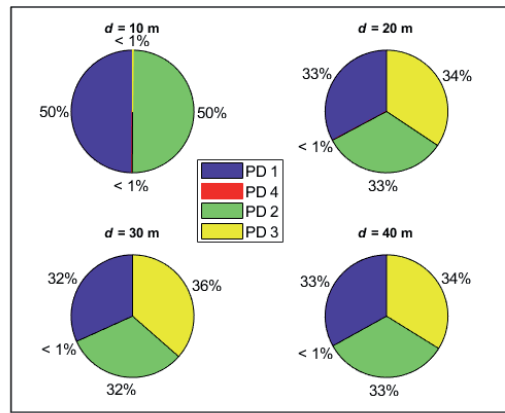


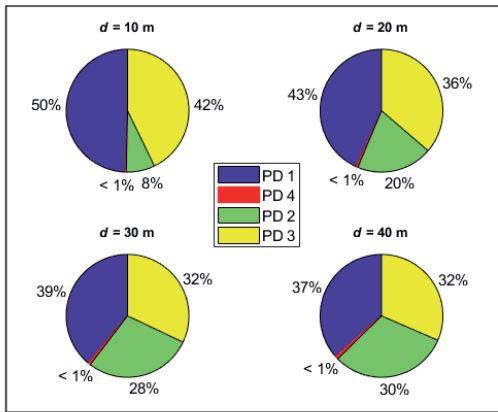
Fig. 5. Received optical power for scenario III (Lane changing).



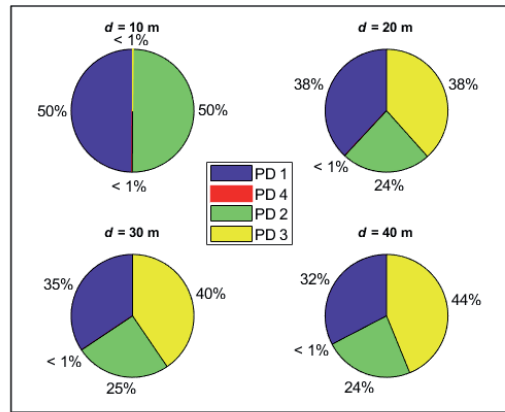
(a) Scenario I



(a) Scenario III, case A



(b) Scenario II



(b) Scenario III, case B

Fig. 4. Power percentage of each PD for Scenarios I and II.

Fig. 6. Power percentage of each PD for all scenarios III.

is observed that the rate of change in the received power during the lane changing range (from 15 m to 30 m) is much higher than that in trailing period (from 30 m to 50 m). This is due to that during the lane switching, there is a change in both inter-vehicle distance ( $d$ ) and horizontal displacement one ( $d_h$ ). It can be also observed from the figure that the starting point of the

lane change can also influence on the received power. For example, consider  $d = 30$  m. The received power considering the starting point at the center of the lane (case A) is -51 dB. For case B where the starting point at the end/edge of the lane, this value is reduced to -53.2 dB.

In Fig. 6, we present pie charts to illustrate the percentage of received powers for Scenario III. We assume the lane changing

occurs from the left-hand side to the right-hand side. It is observed that at the initialization range (from 10 m to 15 m), PD 1 and PD 2 can collect almost all power due to the perfect alignment between the two vehicles. However, during the lane changing range (from 15 m to 30 m), and trailing range (from 30 m to 50 m), PD 3 can collect the highest amount of received power while the contributions of PD 1 and PD 2 are much reduced. It can be also observed in this range (from 15 m to 50 m) that PD 4 is no longer able to receive power. This is due to its location on the other side of the destination vehicle.

#### 4. Conclusions

In this paper, we considered a VLC-based V2V link where the source destination uses high-beam headlights as its transmitters and the destination vehicle is equipped with four PDs. We used non-sequential ray tracing to obtain CIRs and calculate the received power for various practical scenarios including imperfect alignment and lane changes. Our results reveal that two PDs (denoted by PD 1 and PD 2) located at the back of the vehicle under taillights are sufficient to collect almost all power for the perfect alignment case. On the other hand, the other PDs (either PD3 or PD4) become critical when there is imperfect alignment. Our results further reveal that the exact distribution of received power among PDs depend on the inter-distance between vehicles and horizontal displacement. It can be also concluded that four PDs would be sufficient to create the required omni-directional coverage for V2V connectivity. It would be a future research direction whether or not there is a need for additional PDs to enable V2I connectivity.

#### 5. Acknowledgements

The work of Hossien B. Eldeeb has been supported by H2020 Marie Skłodowska-Curie Innovative Training Network (ITN-VisIoN) under Grant 764461. The work of M. Uysal has been supported by the Turkish Scientific and Research Council (TUBITAK) under Grant 215E311.

#### 6. References

- [1] P. H. Pathak, X. Feng, P. Hu, and P. Mohapatra, "Visible light communication, networking, and sensing: A survey, potential and challenges," *IEEE Commun. Surveys Tuts.*, vol. 17, no. 4, pp. 2047–2077, 2015.
- [2] M. Uysal, Z. Ghassemlooy, A. Bekkali, A. Kadri and H. Menouar, "Visible light communication for vehicular networking: Performance study of a V2V system using a measured headlamp beam pattern model," *IEEE Veh. Technol. Mag.*, vol. 10, no. 4, pp. 45-53, Dec. 2015.
- [3] A.-M. Cailean and M. Dimian, "Impact of IEEE 802.15.7 standard on visible light communications usage in automotive applications," *IEEE Commun. Mag.*, pp. 2–7, 2017.
- [4] A. Cailean and M. Dimian, "Current challenges for visible light communications usage in vehicle applications: a survey," *IEEE Commun. Surveys Tuts.*, vol. 19, no. 4, pp. 2681-2703, 2017.
- [5] N. Kumar, D. Terra, N. Lourenco, L. N. Alves, and R. L. Aguiar, "Visible light communication for intelligent transportation in road safety applications", *Proc. IEEE Int. Conf. Wireless Commun. Mobile Computing*, pp. 1513-1518, 2011.
- [6] Y. Bao, Y. Wang, J. Yu, J. Shen, "A visible light communication based vehicle collision avoiding system," *15th Int. Conf. Opt. Commun. and Netw. (ICOON)*, Hangzhou, pp. 1-3, 2016.
- [7] Z. Cui, P. Yue, X. Yi, and J. Li, "Research on non-uniform dynamic vehicle-mounted VLC with receiver spatial and angular diversity," *2019 IEEE Int. Conf. Commun. (ICC)*, May 2019, pp. 1–7.
- [8] B. Turan, G. Gurbilek, A. Uyrus and S. C. Ergen, "Vehicular VLC frequency domain channel sounding and characterization," *IEEE Veh. Netw. Conf. (VNC)*, Taipei, Taiwan, pp. 1-8, 2018.
- [9] M. Elamassie, M. Karbalayghareh, F. Miramirkhani, R. C. Kizilirmak, and M. Uysal, "Effect of fog and rain on the performance of vehicular visible light communications", *IEEE 87th Veh. Technol. Conf. (VTC2018-Spring)*, Porto, Portugal, June 2018.
- [10] D. Schulz, V. Jungnickel, S. Das, J. Hohmann, J. Hilt, P. Hellwig, A. Paraskevopoulos, and R. Freund, "Long-term outdoor measurements using a rate-adaptive hybrid optical wireless/60 GHz link over 100 m," *2017 19th Int. Conf. on Transparent Opt. Netw. (ICTON)*. IEEE, pp. 1–4, 2017.
- [11] H. B. Eldeeb, F. Miramirkhani and M. Uysal, "A Path Loss Model for Vehicle-to-Vehicle Visible Light Communications," *2019 15th Int. Conf. Telecommun. (ConTEL)*, Graz, Austria, 2019, pp. 1-5.
- [12] F. Miramirkhani and M. Uysal, "Channel modeling and characterization for visible light communications," *IEEE Photon. J.*, vol. 7, no. 6, pp. 1–16, 2015.
- [13] Schmidt, S. Kharrazi, S. Erlingsson, C. Van Geem, X. Cocu, and B. Jacob, "Falcon ii: Input for a european pbs definition: Review of vehicle legislations and infrastructure design criteria," *15th International Symposium on Heavy Vehicle Transport Technology: HVTT 15*, Oct 2018, ROTTERDAM, France, 2018.
- [14] Vadeby, G. Sørensen, A. Bolling, X. Cocu, P. Saleh, M. Aleksa, F. La Torre, A. Nocentini, and P. Tucka, "Towards a european guide-line for speed management measures in work zones," *Transportation research procedia*, vol. 14, pp. 3426–3435, 2016.